Solids and Structures (SAS) Volume 5, 2016 www.seipub.org/sas/
doi: 10.14355/sas.2016.05.001

Thick-Walled Open Section Beam and Finite Nodal-Line Method

Yaoqing Gong*[1], Sai Tao[2]

School of Civil Engineering, Henan Polytechnic University, 2oo1 Century Avenue, Jiaozuo City, Henan Province, China

*[1]gongyq@hpu.edu.cn; [2]986107694@qq.com

Abstract

In view of the mechanics problems of the thick-walled open-sectional structural members that cannot be dealt with by existing beam theories, a novel computational methodology named Finite Nodal-Line Method (FNLM) is developed to perform the analysis of the thick-walled open-section beam with a length-aspect ratio less than 3. The computational results coming from an example of L-shaped thick-walled beam have verified the validity of the FNLM.

Keywords

Thick Walled Open Section Beam; Finite Nodal-line Method; Non-uniform Torsion; Torsional Center; Warping Normal Stress

Introduction

With the rapid development of Chinese cities, almost all civil buildings are now built to be tall. In order to expand the utilization of the construction area, and to improve the indoor visual effect and convenient decoration, some new structural systems are widely adopted by the tall buildings such as a frame system with special-shaped columns, a frame shear wall system with special-shaped columns, and etc.. The shape of the cross sections of the special-shaped columns is complicated and the size is not small, some of their limb length close to or more than 1 meters, so that the slenderness ratio (shear span ratio) of the special-shaped column at around 3 or less than 3.

Consequently, a formidable challenge comes out, i.e., the application conditions for all current beam theory do not include tht thick-walled open section beam with a length-aspect ratio less than 3. In addition, due to the inconsistency between the torsional center and geometric centroid of a complex cross section such as channel shaped column, L shaped column, etc., a torsional deformation will be produced under the action of a transverse force without passing through the torsional center. For reinforced concrete material components, the warping normal stress caused by restrained torsion must be particularly concerned. It is just the fatal weakness of existing beam theory, i.e., when a short and thick-walled structural member of complex cross section cannot be freely twisted, the warping stress on the cross section is too hard to be obtained, although there are many beam theories that concern the torsion of a member [1-5].

In order to cope with the challenge, a novel computational methodology named Finite Nodal-Line Method (FNLM) is developed to perform the analysis of the thick-walled beam with a length-aspect ratio less than 3.

Finite Nodal-line Method (FNLM)

The displacement field of a structural member is composed of two parts: the first part is the longitudinal (or axial) displacement, and the second part is the transverse displacement. All the deformed cross sections, which are curved surfaces, are defined to be the longitudinal displacements, and all the torsional rotation angles of each cross section as well as the point set located on the deformed axial line are defined as the transverse displacement of the member. The longitudinal displacement and the lateral displacement together constitute the displacement field of the member.

Without loss of any generality, the displacement field of a thick-walled member can be described by formulating the displacement field of a thick-walled beam with channel cross section as shown in Fig. 1(a).

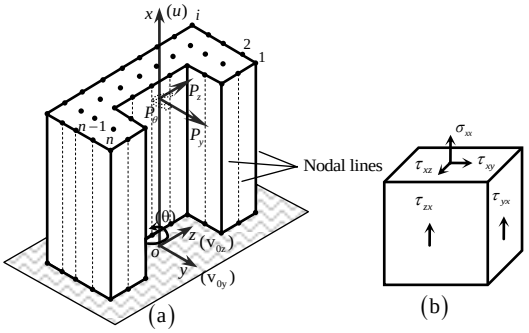

FIG.1: A CHANNEL-SECTION CANTILEVER BEAM
(a) NODAL LINES
(b) STRESS STATE AT AN ARBITRARY POINT

The nodal lines are illustrated in Fig 1(a). If a finite number of unknown functions ($w_i(x)$, $i=1,2,\cdots n$) representing the longitudinal displacements of "n", nodal lines are selected to be basic unknown functions, and interpolation functions ($\varphi_i(y_i,z_i)$, $i=1,2,\cdots,n$) are constructed in between the nodal lines, the longitudinal displacement of the beam can be expressed as follows.

$$u(x,y,z)=\sum w_i(x)\varphi_i(y,z)=\boldsymbol{\Phi}^{\boldsymbol{T}}(y,z)\boldsymbol{W}(x), \tag{1}$$

in which,

$$\boldsymbol{W}(x)=\begin{Bmatrix} w_1(x) \\ w_2(x) \\ \vdots \\ w_n(x) \end{Bmatrix}, \quad \boldsymbol{\Phi}(y,z)=\begin{Bmatrix} \varphi_1(y_1,z_1) \\ \varphi_2(y_2,z_2) \\ \vdots \\ \varphi_n(y_n,z_n) \end{Bmatrix}, \tag{2}$$

where $\boldsymbol{W}(x)$ is the unknown function array of longitudinal displacements, and $\boldsymbol{\Phi}(y,z)$ is the interpolation function array. The domain of $w_i(x)$ is the set of points located along the x-axis; the domain of each $\varphi_i(y_i,z_i)$ is a part area of the cross section enclosed by the connection lines of the node *i* and its nearest neighbors, which are the intersection points between the cross section and nodal lines.

Similarly, if three other basic unknown functions $v_{0y}(x)$, $v_{0z}(x)$, and $\theta(x)$ are chosen to represent the transverse displacements of the beam axis in the *y*-*z* plane and the rotation around the axis *x*, such functions can be expressed as

$$\boldsymbol{V}(x)=\begin{Bmatrix} v_{0y}(x) \\ v_{0z}(x) \\ \theta(x) \end{Bmatrix}. \tag{3}$$

The domain of the three unknown functions is the point set located on the beam axis.

By means of the displacement field defined in equations (1) and (3), the displacement of an arbitrary point in the beam in the x, y, and z directions can be expressed as follows.

$$\left.\begin{aligned} u(x,y,z)&=\boldsymbol{\Phi}^{\boldsymbol{T}}(y,z)\boldsymbol{W}(x) \\ v_y(x,z)&=v_{0y}(x)-z\theta(x) \\ v_z(x,y)&=v_{0z}(x)+y\theta(x) \end{aligned}\right\}. \tag{4}$$

As a result, **the state of strain at an arbitrary point** in the beam can be expressed in terms of equation (4) as

$$\boldsymbol{\varepsilon}=\begin{Bmatrix} \varepsilon_{xx}=u_{,x} & \gamma_{xy}=v_{y,x}+u_{,y} & \gamma_{xz}=v_{z,x}+u_{,z} \\ \gamma_{yx}=u_{,y}+v_{y,x} & \varepsilon_{yy}=v_{,y} & \gamma_{yz}=v_{z,y}+v_{y,z} \\ \gamma_{zx}=u_{,z}+v_{z,x} & \gamma_{zy}=v_{y,z}+v_{z,y} & \varepsilon_{zz}=v_{,z} \end{Bmatrix}. \tag{5}$$

In the above, the comma indicates a partial derivative with respect to the coordinate that follows.

Generally, when a beam is subjected to arbitrary loading, the normal stress in its longitudinal (axial) direction is much larger than those in its transverse directions. The stress state at an arbitrary point in the beam should be as shown in Fig. 1 (b), a space stress state with zero normal stress σ_{yy} and σ_{zz} as well as zero shear stress τ_{yz}. Fortunately, the strain state is matched, as shown in equation (5), $\varepsilon_{yy}=\varepsilon_{zz}=\gamma_{yz}=\gamma_{zy}=0$.

Also without loss of any generality, let us consider that the beam shown in Fig. 1 (a) is subjected to two concentrated loads, P_y and P_z, in the y and z directions, respectively, and a concentrated couple, P_θ, around the axis *x*, at the top end of the beam. This problem becomes a spatial cantilever beam subjected to static loads. Using equation (5) and Hook's law between stresses and strains of an elastic member with small deformations, the elastic potential energy of the beam is given by

$$\Pi=\int_0^L dx\iint_\Omega \frac{1}{2}(\sigma_{xx}\varepsilon_{xx}+\tau_{xy}\gamma_{xy}+\tau_{zx}\gamma_{zx})dydz\,, \tag{6}$$

in which, Ω is the cross-sectional area in the *yoz* plane.

The work done by non-conservative forces is

$$W_{nc}=P_y v_{0y}(L)+P_z v_{0z}(L)+P_\theta\theta(L)\,, \tag{7}$$

where *L* is the length of the beam.

The **governing equations** under these loading conditions will be obtained by resorting to the minimum potential energy condition, i.e. $\delta(\Pi-W_{\mathrm{nc}})=0$. This leads to the following.

$$\left.\begin{aligned} \boldsymbol{A}\boldsymbol{W}''(x)-\boldsymbol{B}\boldsymbol{W}(x)-\boldsymbol{C}\boldsymbol{V}'(x)=\boldsymbol{0} \\ \boldsymbol{D}\boldsymbol{V}''(x)+\boldsymbol{C}^{\boldsymbol{T}}\boldsymbol{W}'(x)=\boldsymbol{0} \end{aligned}\right\}, \tag{8}$$

In which, $\mathbf{0}$ is a zero array, and

$$\mathbb{A}=\iint_\Omega E\boldsymbol{\Phi}(y,z)\boldsymbol{\Phi}^{\mathrm{T}}(y,z)dydz\,, \qquad \boldsymbol{B}=\iint_\Omega G\frac{\partial\boldsymbol{\Phi}(y,z)}{\partial y}\frac{\partial\boldsymbol{\Phi}^{\boldsymbol{T}}(y,z)}{\partial y}dydz+\iint_\Omega G\frac{\partial\boldsymbol{\Phi}(y,z)}{\partial z}\frac{\partial\boldsymbol{\Phi}^{\boldsymbol{T}}(y,z)}{\partial z}dydz\,,$$

$$\mathbb{C}=\begin{Bmatrix} \iint_\Omega G\dfrac{\partial\boldsymbol{\Phi}(y,z)}{\partial y}\mathbb{T}_1 dydz+\iint_\Omega G\dfrac{\partial\boldsymbol{\Phi}(y,z)}{\partial z}\mathbb{T}_2 dydz \\ +\iint_\Omega G(y\dfrac{\partial\boldsymbol{\Phi}(y,z)}{\partial z}-z\dfrac{\partial\boldsymbol{\Phi}(y,z)}{\partial y})\mathbb{T}_3 dydz \end{Bmatrix}, \qquad \boldsymbol{D}=\begin{bmatrix} \iint_\Omega Gdydz & 0 & -\iint_\Omega Gzdydz \\ 0 & \iint_\Omega Gdydz & \iint_\Omega Gydydz \\ -\iint_\Omega Gzdydz & \iint_\Omega Gydydz & \iint_\Omega G(y^2+z^2)dydz \end{bmatrix},$$

$$\boldsymbol{P}=\begin{Bmatrix} P_y \\ P_z \\ P_\theta \end{Bmatrix}, \qquad \begin{aligned} \mathbb{T}_1&=[1,0,0] \\ \mathbb{T}_2&=[0,1,0]. \\ \mathbb{T}_3&=[0,0,1] \end{aligned}$$

The **boundary conditions** corresponding to equation (8) are

$$\text{at } x=0, \quad \begin{cases} \boldsymbol{W}(0)=\boldsymbol{0} \\ \boldsymbol{V}(0)=\boldsymbol{0} \end{cases}, \tag{9}$$

$$\text{at } x = L, \quad \begin{cases} \boldsymbol{AW}'(L) = \boldsymbol{0} \\ \boldsymbol{DV}'(L) + \boldsymbol{C}^T \boldsymbol{W}(L) - \boldsymbol{P} = \boldsymbol{0} \end{cases}. \tag{10}$$

Equation (8), as well as its corresponding boundary conditions, (9) and (10), constitute a boundary value problem of ordinary differential equations, and its numerical solutions can be obtained by an Ordinary Differential Equation Solver (ODE Solver) [6-7], which is of high quality and high efficiency, known as the numerical analytical solution.

Numerical Examples and Results

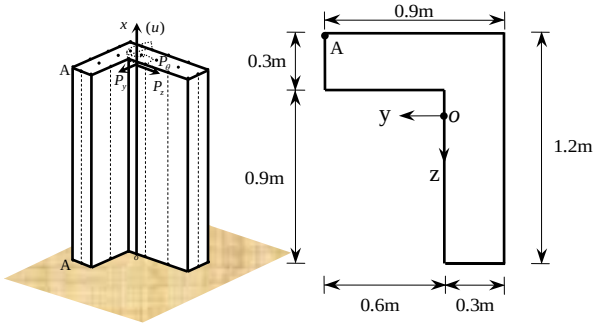

FIG. 2 AN L-SHAPED BEAM AND ITS CROSS SECTION

Figure 2 shows the cross section of an L-shaped cantilever beam of a length $l = 3.0\text{m}$. The Young's modulus of the material $E = 3.0\times10^{10}\,\text{Pa}$ and the shear modulus $G = 1.22\times10^{10}\,\text{Pa}$. Other dimensions of the cross section are shown in the figure. In order to investigate the mechanical caracteristics of non uniforme torsion, non-symmetric bending, and coupling action of non-symmetric bending and torsion for the special thick-walled open section beam, respectively, three loading conditions are considered.

Loading Condition 1: a concentrated torque $P_\theta = 500\text{kN}\cdot\text{m}$ is applied at the free end; Loading Condition 2: a transverse concentrated force of 100kN towards the z direction is applied and passed through its geometric center at the free end; Loading Condition 3: a force of 200kN in the y direction and a force of 100kN in the z direction passed through its geometric center, and a counter clockwise torque of $500\text{kN}\cdot\text{m}$ around the x axis are loaded at the free end.

By means of the FNLM, the governing equations and corresponding boundary conditions of the L-section beam are identical to equtions (8) to (10) for the three loading conditions, except that the loading array in eqution (10) will respectively become

$$\text{Condition 1: } \boldsymbol{P} = [0.0 \quad 0.0 \quad 500.0\times10^3]^T,$$

$$\text{Condition 2: } \boldsymbol{P} = [0.0 \quad 100.0\times10^3 \quad 0.0]^T,$$

$$\text{Condition 3: } \boldsymbol{P} = [200.0\times10^3 \quad 100.0\times10^3 \quad 500.0\times10^3]^T.$$

The boundary-value problem formulated by equations (8) to (10) with the above loading condition can be solved by ODE Solver. The stiffness matrices **A**, **B**, **C** and **D** can be determined by the size and the elastic modulus of the cross section of the example; the centroid coordinates can be determined to be at position (0.3m from long side, 0.45m from short side), needed for the determination of the stiffness matrices.

Table 1 presents the normal stress at different position of nodal line A-A and warping displacements of different cross sections due to the restraint torsion; Table 2 shows deflections in the y and z directions, and torsional angles around the x axis (counter clockwise positive) at different cross sections of the beam due to the restrained torsion; Table 3 indicates deflections in the y and z directions, and torsional angles at different cross sections of the beam due to the transverse force towards the z direction.

Figures 3, 4, and 5 display the axial deformations of the cross-section at x=1.5m due to the non-uniform torsion, the non-symmetric bending and the coupling action of non-symmetric bending and torsion, which are respectively depicted by the FNLM numerical solutions.

TABLE 1 THE WARPING STRESS AND WARPING DISPLACEMENT OF THE NODAL LINE A-A AT DIFFERENT SECTIONS DUE TO NON-UNIFORM TORSION

x/m	$\sigma(x)$/MPa	$w(x)$/ m
0.00	10.06	0.00
0.75	1.92	1.30×10^{-4}
1.50	0.33	1.52×10^{-4}
3.00	0.00	1.57×10^{-4}

TABLE 2 THE DEFLECTIONS AND TORSIONAL ANGLES OF L-SHAPED BEAM AT DIFFERENT SECTIONS DUE TO NON-UNIFORM TORSION

x/m	$v_{0y}(x)$ /m	$v_{0z}(x)$ / m	$\theta(x)$ /rad
0.00	0.00	0.00	0.00
0.75	-2.39×10^{-4}	1.46×10^{-4}	1.19×10^{-3}
1.50	-6.61×10^{-4}	4.01×10^{-4}	3.01×10^{-3}
3.00	-1.58×10^{-3}	9.51×10^{-4}	6.88×10^{-3}

TABLE 3 THE DEFLECTIONS AND TORSIONAL ANGLES OF L-SHAPED BEAM AT DIFFERENT SECTIONS DUE TO THE FORCE ALONG THE Z AXIS

x/m	$v_{0y}(x)$ /m	$v_{0z}(x)$ / m	$\theta(x)$ /rad
0.00	0.00	0.00	0.00
0.75	3.14×10^{-5}	7.18×10^{-5}	2.93×10^{-5}
1.50	1.19×10^{-4}	2.32×10^{-4}	8.02×10^{-5}
3.00	3.97×10^{-4}	6.93×10^{-4}	1.90×10^{-4}

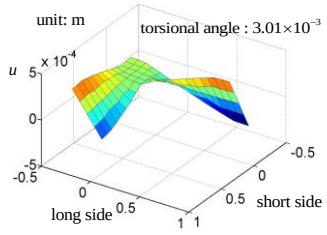

FIG. 3 THE CROSS-SECTIONAL AXIAL WARPING DUE TO NON-UNIFORM TORSION

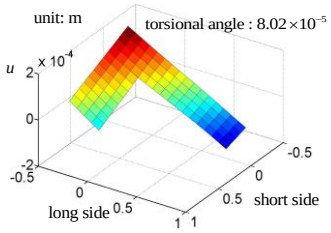

FIG. 4 THE CROSS-SECTIONAL AXIAL WARPING DUE TO NON-SYMMETRIC BENDING

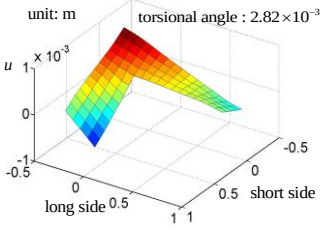

FIG. 5 CROSS-SECTIONAL AXIAL WARPING DUE TO NON-SYMMETRIC BENDING AND TORSION

Conclusions

The maximum warping normal stress caused by pure restrained torsion will occur at the fixed end of the cantilever beam, while the maximum warping displacement induced by pure restrained torsion will appear on the cross

section at the free end of the beam, as shown in Table 1.

When an L-shaped cantilever beam is subjected to restrained torsion, not only the torsional angles around x axis will be produced, but also the deflections both along the y direction and z direction will be generated as shown in Table 2. This indicates that an L-shaped thick-walled beam also has a shear center (torsional center), i.e., when a torque is not applied around the shear-centers connected line, both the torsional and bending deformations will be induced by the torque.

When an L-shaped cantilever beam is subjected to a transverse force along the z axis, not only the deflection in the z direction will be yielded, but also the deflection in the y direction and torsional angle around x axis will be developed as shown in Table 3. This phenomena again shows that an L-shaped thick-walled beam has the shear center (or torsional center); the phenomena also demonstrates the characteristics of non-symmetric bending, i.e., when the load surface is inconsistent with the main centroidal inertial plane of the cross-section of a beam, the bending deflections will be produced in two directions.

The cross section of a thick-walled beam with an aspect ratio less than 3 will be warping to a curved surface as shown in Fig. 3, 4 and 5, whenever it is under the action of a combination of bending and restrained torsion, restrained torsion alone, or non-symmetric bending alone. Especially, under restrained torsion alone, the cross sectional warping of an L-shaped cantilever is more obvious, and the warping normal stress due to restrained torsion (see Table 1) must be taken into consideration.

ACKNOWLEDGMENT

The research work was supported by the Natural Science Foundation of China (51178164) and the Priority Discipline Foundation of Henan Province (60705/004).

REFERENCES

[1] Saint-Venant, de, A.J.C.B. “Mémoire sur la flexion des prismes.” Journal de Mathématiques Pures et Appliquées 1 (2), 89–189, 1856.

[2] Vlasov VZ. “Thin-walled elastic beams.” Jerusalem: Monson; 1961.

[3] Schardt RP. “Generalized beam theory—an adequate method for coupled stability problems.” Thin-Walled Structures; 19, 161–80, 1994.

[4] Rached El Fatmi. “Non-uniform warping including the effects of torsion and shear forces. Part I: A general beam theory.” International Journal of Solids and Structures, 44, 5912–5929, 2007.

[5] Stefano de Miranda, Antonio Madeo, Rosario Miletta, Francesco Ubertini. “On the relationship of the shear deformable Generalized Beam Theory with classical and non-classical theories.” Thin-Walled Structures, 51, 3698–3709, 2014.

[6] Ascher U, Christiansen J, Russell RD. “Collocation Software for Boundary-Va1ue ODEs.” ACM Trans Math Software, 7(2), 209-222, 1981.

[7] Yuan S. “ODE conversion techniques and their applications in computational mechanics.” Acta Mechanica Sinica, 7(3), 283–288, 1991.